THE JOURNAL OF PHYSICAL CHEMISTRY B

Article

pubs.acs.org/JPCB

Supramolecular Polymerization of Benzene-1,3,5-tricarboxamide: A Molecular Dynamics Simulation Study

Karteek K. Bejagam,[†] Giacomo Fiorin,[‡] Michael L. Klein,[‡] and Sundaram Balasubramanian*[,†]

[†]Chemistry and Physics of Materials Unit, Jawaharlal Nehru Centre for Advanced Scientific Research, Bangalore 560 064, India

[‡]Institute for Computational Molecular Science, Temple University, Philadelphia, Pennsylvania 19122, United States

Supporting Information

ABSTRACT: Supramolecular polymerization in the family of benzene-1,3,5-tricarboxamide (BTA) has been investigated using atomistic molecular dynamics (MD) simulations. Gas phase calculations using a nonpolarizable force field reproduce the cooperativity in binding energy and intermolecular structure seen in quantum chemical calculations. Both quantum chemical and force field based calculations suggest that the ground state structure of the BTA dimer contains two donor hydrogen bonds and one acceptor hydrogen bond rather than the conjectured three-donor and zero-acceptor hydrogen-bonded state. MD simulations of BTA molecules in a realistic solvent, *n*-nonane, demonstrate the self-assembly process. The free energy (FE) of dimerization and of solvation has been determined. The solvated dimer of BTA with hexyl tails is more stable than two monomers by about 13 kcal/mol. Furthermore, the FE of association of a BTA molecule to an oligomer exhibits a dependence on the oligomer size, which is a robust signature of cooperative self-assembly.

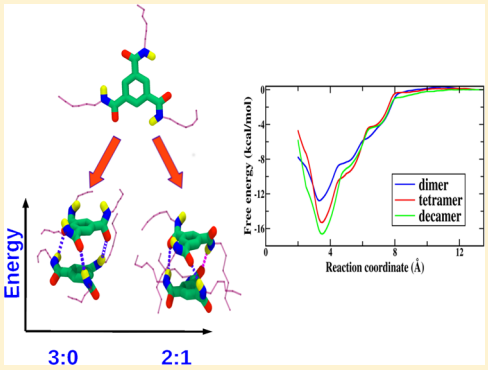

INTRODUCTION

The self-assembly of molecules in solution guided through noncovalent interactions such as $\pi-\pi$, van der Waals, hydrophobic, dipole−dipole, and hydrogen bonding is a subject of considerable interest.[1] Control over the extent and nature of aggregation by means of functional groups, temperature, light, and solvent enables the assemblies to function as liquid crystals,[2] organogelators,[3] light harvesters,[4] ferroelectric switches,[5] etc. Discotic molecules self-assemble into one-dimensional columnar aggregates[6−8] and further interact to form fibers; with appropriate functional groups, they can form pyramidal columns and chiral spheres.[9] Percec et al. studied the assembly of dendronized perylene bisimides as a function of methylenic spacers into various columnar phases.[10] Addition of chiral molecules into an achiral solution has been shown to induce chiral amplification.[11−13] Further, a chiral guest can induce chirality in achiral assemblies, thus providing a handle to tune the preferred organization.[14]

In a variety of one-dimensional supramolecular polymeric systems, self-assembly proceeds via two principal mechanisms—cooperative or isodesmic.[15] Experimentally, these mechanisms are distinguished using mainly UV/visible absorption spectroscopy and circular dichroism either as a function of temperature or concentration of the solute. Isodesmic systems exhibit a sigmoidal curve for the fraction of aggregates, while cooperative ones show a sharp rise at a specific temperature or concentration. Gas phase quantum chemical calculations demonstrate that the interaction energy between two molecules following the cooperative pathway shows a dependence on the oligomer size prior to saturation,[16,17] while, in the isodesmic case, the interaction energy is independent of oligomer size. Concurrently, many geometrical parameters (hydrogen bond lengths, $\pi-\pi$ distance, etc.) also exhibit either a dependence on oligomer size or not. The cooperative mechanism could involve a nucleation and growth process resulting in the formation of a few, large aggregates in solution at equilibrium, while the isodesmic one results in many smaller aggregates. The manner in which molecular details determine the mechanism of assembly has not been unequivocally ascertained yet; however, it has recently been conjectured that the presence of functional groups in a molecule which can enable long-range interactions between its oligomers along the stacking direction can lead to cooperative behavior and the lack of such specific moieties to the isodesmic case.[18]

One of the molecules studied extensively in supramolecular chemistry is benzene-1,3,5-tricarboxamide (BTA), with a C_3 symmetric structure around a benzene ring core, as shown in Figure 1. BTA, with pentyl or longer alkyl tails, exhibits a liquid crystalline phase.[2] The self-assembly of BTA and compounds derived from it in apolar solvents such as heptane and methylcyclohexane have been extensively studied by Meijer and co-workers.[11,19−24] BTA exists in monomeric form at high temperature and self-assembles in a cooperative fashion upon

Received: March 20, 2014
Revised: April 26, 2014
Published: April 29, 2014

   dx.doi.org/10.1021/jp502779z | J. Phys. Chem. B 2014, 118, 5218−5228

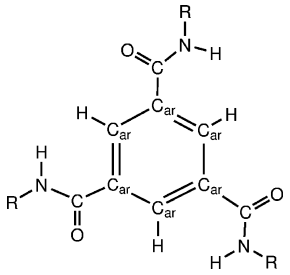

Figure 1. Benzene-1,3,5-tricarboxamide. **1a**, R = H; **1b**, R = $-(CH_2)_2CH_3$; **1c**, R = $-(CH_2)_5CH_3$.

cooling to yield one-dimensional, helical columnar stacks. Although the monomer is planar and hence has zero dipole moment, intermolecular C═O···H—N hydrogen bonds between molecules present in an oligomer necessitate the amide and the carbonyl groups of a given molecule to orient themselves in opposite directions of the molecular plane, thus generating a molecular dipole moment. As the dipoles of individual molecules are oriented along the same direction, the magnitude of the total dipole moment of the stack (a macrodipole) increases with stack size. Stacks have been conjectured to interact via dipole−dipole forces to result in fibers.[25]

Despite the large number of experimental studies on supramolecular polymers and a good number devoted to their mechanisms of assembly, there have been only a few theoretical studies. Gas phase quantum chemical calculations have shown the specific interactions responsible for oligomerization. Accurate calculations are prohibitively expensive due to the large number of atoms in a BTA molecule, and are thus limited to oligomers not exceeding a dodecamer.[16,25] Cooperativity has been demonstrated in hydrogen bond lengths, torsional angles, and binding energies. However, these gas phase zero Kelvin calculations need to be supplemented by finite temperature simulations which include the solvent as well. Molecular dynamics (MD) is a powerful tool to explore the self-assembly at the molecular level.[26−32] Force field based MD simulations have been carried out to model supramolecular systems including a C_3 symmetric BTA based compound,[33] anionic azo dye,[34] and bis-urea.[35] MD simulations can reveal aggregation mechanisms, structural details, the relative importance of various interactions, energetics, and temperature effects on columnar stacking. In this article, we provide results of atomistic MD simulations of BTA in a solvent of *n*-nonane. In anticipation of our results, we provide microscopic details of stack formation, signatures of cooperativity, and the role played by the dipole moment of the hydrogen bond in the structure of a column. The MD simulations have also been augmented by quantum chemical calculations to determine the exact configuration of hydrogen bond dipoles in oligomers. We have also determined the free energies of solvation and dimerization of these molecules in solution and have investigated self-assembly into stacks. The dynamics of preformed stacks have also been investigated.

■ COMPUTATIONAL DETAILS

The DREIDING force field[36] is employed to describe BTA molecules. In addition to a specific hydrogen bonding potential term, the force field offers specific potential types in which the atomic sites either contain a partial charge or not, hereinafter referred to as DREIDING-C and DREIDING-N, respectively. In the former, Gasteiger charges[37] are identified on atomic sites.

$$E = \sum^{\text{bond}} K_r(r - r_o)^2 + \sum^{\text{angle}} K_\theta(\theta - \theta_o)^2 + \sum^{\text{dihedral}} K(1 - \cos[n(\phi - \phi_o)]) + \sum^{\text{inversion}} K(1 - \cos\phi) + E_{nb} \quad (1)$$

$$E_{nb} = E_{vdW} + E_Q + E_{hb}, \quad \text{where}$$

$$E_{vdW} = A\exp(-Cr_{ij}) - B/r_{ij}^6$$

$$E_Q = q_i q_j/(4\pi\varepsilon_o r_{ij})$$

$$E_{hb} = D_{hb}[5(R_{hb}/R_{DA})^{12} - 6(R_{hb}/R_{DA})^{10}]\cos^4(\theta_{DHA}) \quad (2)$$

E_{hb} is a three-body term that is used to describe hydrogen bond interactions.

In our simulations, BTA molecules were considered in an all-atom representation. All the simulations were performed with the MD program LAMMPS[38] at a temperature of 298.15 K maintained through the use of a Nóse−Hoover chain thermostat[39] with a coupling constant of 1 ps. Three-dimensional periodic boundary conditions were applied on either cubic or orthorhombic boxes depending on the nature of the system. Nonbonded interactions were truncated at 12 Å. Long-range Coulombic interactions were treated using the particle−particle particle−mesh (PPPM)[40] solver. Long-range corrections to energy and pressure were applied. Full scaling of 1−4 interactions was employed. Free energy calculations were carried out with a time step of 0.5 fs using the velocity Verlet algorithm with *n*-nonane as solvent, and the latter was modeled using the all-atom DREIDING-N model. In regular MD simulations (i.e., ones which did not involve free energy calculations), the TRaPPE united atom model[41] of *n*-nonane was employed to reduce computational cost. Cross interactions between BTA and solvent were handled using DREIDING's mixing rules. In these runs, the multiple time step method, r-RESPA,[42] was employed. The outer time step was 1 fs, while all bond stretches were integrated with a time step of 0.5 fs. VMD[43] was used for visualization.

Adaptive Biasing Force (ABF). Free energy (FE) calculations have been employed in a variety of problems—to determine stable structures, to overcome barriers, and in particular to predict the energy difference between two states. Herein, FE profiles are obtained using the "colvars" (collective variable) module[44,45] integrated with LAMMPS. Adaptive biasing force (ABF) is a FE technique which employs the application of an external force on the system to explore the configurational space. In the ABF method, the force experienced on the reaction coordinate (RC) is averaged over a given number of steps ($N_{samples}$). ABF applies an external biasing force (F_{ABF}), which is exactly opposite to this average force $\langle F \rangle$, so as to smoothen the potential surface for uniform sampling. The full window of the RC is divided into smaller bins in each of which accumulation of force takes place. The width of each bin should be small enough to capture the variations in FE but large enough to permit good statistics. In our simulations, the total RC was divided into nonoverlapping windows to improve the sampling and the convergence of FE. The initial configurations for these windows were obtained

dx.doi.org/10.1021/jp502779z | J. Phys. Chem. B 2014, 118, 5218−5228

Table 1. Comparison of Geometries of BTA Oligomers Optimized in the Gas Phase Using the DREIDING Force Field and Quantum Density Functional Theory[a]

oligomer size (n)	stacking distance (Å)	hydrogen bond distance (Å)	O−C−C_{Ar}−C_{Ar} dihedral angle (deg)	H−N−C_{Ar}−C_{Ar} dihedral angle (deg)	binding energy (kcal/mol)	dipole moment per molecule[b] (D)
			DREIDING-N			
2	3.44	1.84	36.9	38.2	−30.1	4.42
3	3.44	1.84	43.4	40.3	−30.9	4.50
5	3.45	1.84	42.2	39.1	−31.3	4.63
6	3.44	1.84	42.3	39.2	−31.4	4.65
10	3.44	1.84	42.2	39.1	−31.5	4.64
			DREIDING-C			
2	3.31	1.89	9.4	35.6	−17.9	2.36
3	3.31	1.87	25.3	41.4	−19.6	2.91
5	3.31	1.86	24.4	39.8	−20.7	3.33
6	3.31	1.85	24.6	39.8	−21.0	3.43
10	3.32	1.85	24.8	39.9	−21.5	3.64
15	3.32	1.85	24.9	40.1	−21.7	3.75
20	3.32	1.85	24.9	40.0	−21.9	3.80
30	3.29	1.86	24.8	39.4	−22.0	3.83
40	3.33	1.85	25.0	40.2	−22.0	3.86
50	3.33	1.85	25.0	40.3	−22.0	3.89
			PBE+vdW[16]			
	3.72	1.82	36.8[46]	42.4[46]	−27.1	12.35

[a]Binding energy is defined as $(E_n - nE_1)/(n-1)$, where E_n is the energy of an oligomer of size n. Geometrical parameters pertain to the core region of an oligomer. [b]Dipole moments of oligomers optimized with DREIDING-N were calculated using DREIDING-C charges.

from steered molecular dynamics (SMD) simulations. Jacobian terms were included in all of the FE calculations.

Dimerization Free Energy (DFE). DFE represents the FE for the formation of a dimer from two separated monomers present either in gas phase or in solution, at a given temperature. Here, the RC is defined as the distance between the center of mass of the two molecules, excluding their alkyl groups.

Gas Phase. Two BTA molecules in their dimerized state were placed in a cubic box of edge length 100 Å, large enough to avoid image interactions. The total RC, spanning from 2.5 to 26.5 Å was divided into four nonoverlapping windows. $N_{samples}$ was chosen to be 200, and the bin width was set to 0.1 Å. The biasing force was obtained as an average over 200 steps.

Bulk Phase. Two BTA molecules in their dimerized state were solvated in a pre-equilibrated box containing n-nonane molecules. Molecules of the solvent having hard contacts with the solute were removed. The RC was split into four nonoverlapping windows, each of 3.5 Å width so as to span the distance from 2.5 to 16.5 Å. $N_{samples}$ was chosen to be 1000 so as to provide sufficient time for the solvent molecules to equilibrate. The bin width to accumulate the force was chosen to be 0.1 Å. Simulations were carried out in the constant isothermal−isobaric (NPT) ensemble.

Solvation Free Energy (SFE). 150 n-nonane molecules were equilibrated in a cubic box under constant NPT conditions. The box length along the z-direction was later increased to 200 Å which created two liquid−vapor interfaces. Simulations to calculate the SFE of BTA in this solvent were performed subsequently in the canonical (NVT) ensemble. The RC was defined as the distance between the center of mass of all the nonane molecules and the lone BTA molecule (excluding its alkyl tails). The span of RC was chosen sufficiently large to ensure that the molecule was completely immersed in the solvent at one end and completely in the vacuum at the other end of the RC. SFE is the difference in energy between the two plateaus. The RC spanned from 0 Å (center of nonane box) to 45 Å and was divided into five nonoverlapping windows each of width 9 Å. The colvar style of "distanceZ" was used to apply the force normal to the liquid surface. The ABF parameters used were 1000 for $N_{samples}$ and 0.2 Å for bin width.

RESULTS AND DISCUSSION

Gas Phase Oligomers: Comparison between Force Field and Quantum Data. As mentioned before, the monomer of **1a** is planar, while, in an oligomer, the oxygen and amide hydrogens of a given molecule are oriented toward either side of the benzene plane, to form three intermolecular hydrogen bonds. The geometries of oligomers of **1a** in the gas phase, optimized with the DREIDING force field, are compared in Table 1 against those determined by quantum chemical calculations performed by us earlier.[16] Values of the hydrogen bond distance, $\pi-\pi$ stacking distance, dihedral angles of the central core, binding energies, and the mean dipole moment per molecule of the oligomer are also provided. The latter was calculated as the ratio of the total dipole moment (macrodipole) of the oligomer to the oligomer size. Both DREIDING-C and DREIDING-N are able to provide a good account of many geometrical parameters. However, DREIDING-N slightly overestimates and DREIDING-C underestimates the binding energy compared to quantum chemical results. Interestingly, DREIDING-C, despite being a nonpolarizable force field, is able to demonstrate cooperativity in the dependence of binding energy per molecule on stack size (Figure 2). Cooperativity was also observed across dihedral, hydrogen bond, Coulombic, and van der Waals energies (data not shown). The binding energy of the stack converges to values of −22.1 and −31.6 kcal/mol using the DREIDING-C and DREIDING-N force fields, respectively, in comparison to a value of −27.1 kcal/mol obtained using PBE+vdW.[16]

dx.doi.org/10.1021/jp502779z | J. Phys. Chem. B 2014, 118, 5218−5228

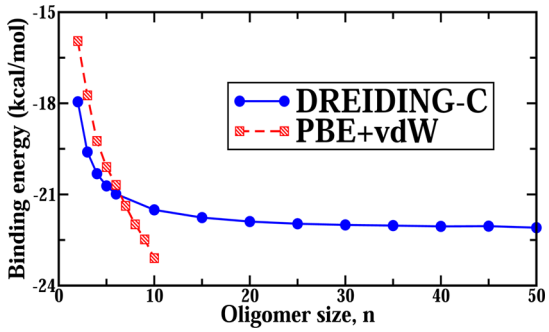

Figure 2. Binding energy (see Table 1 for definition) of geometry optimized oligomers as a function of their size *n*, obtained using the DREIDING-C force field and the PBE+vdW level of theory.[16]

Columnar Stack in Solvent: Stability. Prior to the exploration of self-assembly of BTA molecules, we need to evaluate the capability of the force field in maintaining the stability of a prebuilt columnar stack in bulk solvent at a finite temperature. Toward this purpose, a MD simulation of a 3-fold hydrogen bonded oligomer (of size 20) of **1c**, solvated in *n*-nonane, was carried out at 298.15 K for a duration of 10 ns using both the DREIDING-C and DREIDING-N force fields. Configurations were saved every 5 ps for visualization and analyses. All hydrogen bonds were found to be intact throughout the simulation in both the runs, implying that the force field adopted here could reasonably represent this system. Figure 3a exhibits a typical snapshot of this 20-mer near the end of this run. Three BTA molecules present within this stack are highlighted in Figure 3b.

Cooperativity in Bulk Solvent. MD simulations of oligomer stacks of various sizes, each solvated in a box containing 5457 *n*-nonane molecules, were carried out at 298.15 K. In all, simulations of 13 different stacks (of 3:0 type) were carried out. Each system was simulated under constant NPT conditions for at least 3 ns. In a given configuration along the MD run, the potential energy of each BTA molecule was calculated as the sum of its interaction energy with other BTA molecules and with those of the solvent. The value was then averaged over all the BTA molecules in the stack. The mean potential energy of a molecule in a stack is plotted against oligomer size in Figure 4. Such simulations, carried out under bulk conditions and at finite temperature, are a more robust check of cooperative behavior of self-assembly than gas phase, zero Kelvin calculations. The potential energy per molecule of a BTA stack displays a dependence on the oligomer size prior to saturation, illustrating the cooperative behavior of aggregation as seen in Figure 4. In fact, in a large enough stack, the potential energy of a molecule present in the core of the stack is more negative (i.e., more stabilized) than for one present in its periphery (data not shown). This too is evidence of cooperativity.

Supramolecular Aggregation. To understand the mechanism of self-assembly, we solvated 10 molecules of **1c** in a box containing 1500 *n*-nonane molecules. The initial configuration contained BTA molecules placed randomly in this simulation box, using PACKMOL.[47] MD simulations were performed under constant NPT conditions at 298.15 K and 1 atm, and coordinates were saved every 5 ps. A few snapshots illustrating the self-assembly process are shown in Figure 5. The monomers self-assemble to form small oligomers which coalesce to form a longer hexagonal columnar stack. Earlier

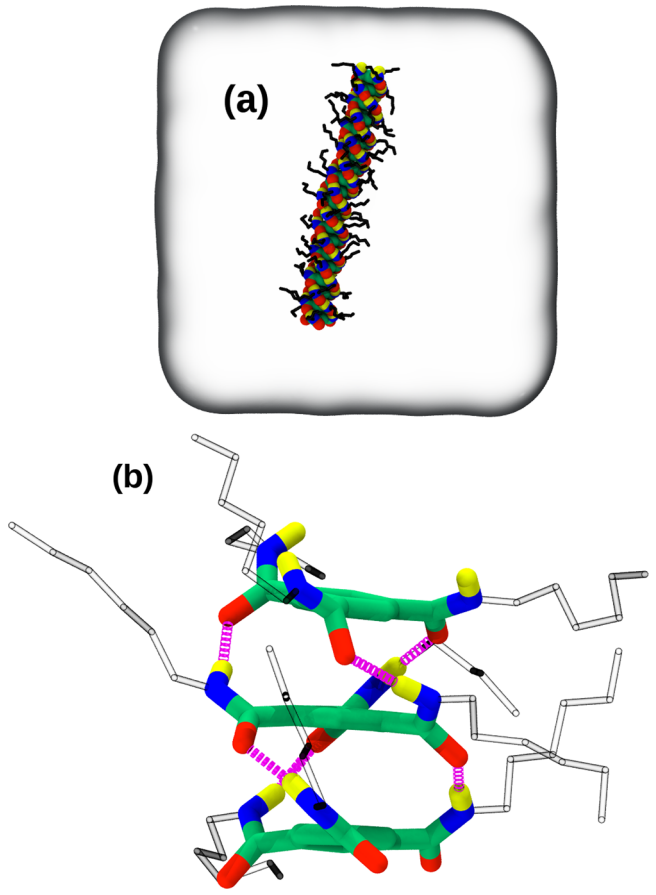

Figure 3. (a) Snapshot of a 20-mer of **1c** solvated in *n*-nonane at 298.15 K taken from a MD run employing the DREIDING-C force field. (b) Three adjacent molecules taken from the center of the stack. Hydrogens on the alkyl tails are not shown for clarity. Color scheme: carbon, green; oxygen, red; nitrogen, blue; hydrogen, yellow; carbon (tail), black. Dashed lines are hydrogen bonds. Note the opposite orientations of the carbonyl oxygens and amide hydrogens of a given molecule, with respect to the molecular plane. Intermolecular hydrogen bonds thus formed are aligned along the stack direction, imparting a macrodipole to the stack. The directions of the hydrogen bond dipole moment vector and that of the macrodipole of the stack are opposite to each other.

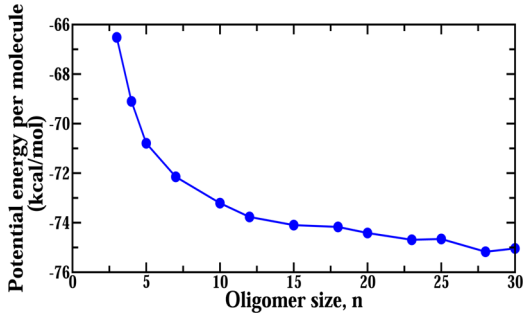

Figure 4. Cooperativity exhibited by mean potential energy per BTA molecule of oligomers solvated in bulk *n*-nonane at 298.15 K.

experiments[6,48] and computations[16,49] have proposed that the stacks are constituted by molecules whose NH groups are all oriented in one direction and the carbonyl oxygen atoms in the other direction, with respect to the benzene plane.

However, in our MD simulations, the molecules in the stack were found to have two amide NH groups and one carbonyl

dx.doi.org/10.1021/jp502779z | J. Phys. Chem. B 2014, 118, 5218−5228

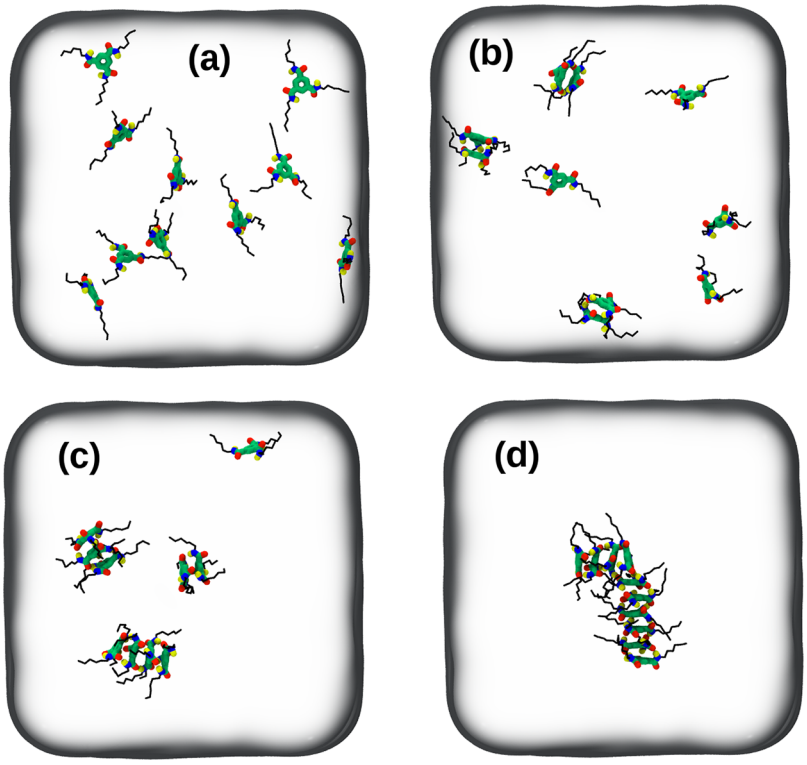

Figure 5. Snapshots exhibiting the progress of supramolecular self-assembly of **1c** in *n*-nonane starting from a random configuration at (a) 0 ns, (b) 2 ns, (c) 6.5 ns, and (d) 70 ns, respectively, studied using the DREIDING-C force field. The color scheme is the same as that in the previous figure.

oxygen to be oriented along the same direction. Thus, each molecule participates in three intermolecular hydrogen bonds in a given direction; two of them are of donor type and one of acceptor type (or vice versa). At first sight, it may appear that this configuration may be metastable with respect to the one in which all acceptor hydrogen bonds of a molecule are oriented along the same direction. However, we observe (see later) that this configuration is indeed more stable than the one in which all three amide NH groups form hydrogen bonds with the same molecule adjacent to it in the stack.

For now, let us define the configurations as follows:

(i) Symmetric: Three amide NH groups of a molecule oriented along the same direction (hereinafter referred to as 3:0). A dimer of this type is shown in Figure 6a.

(ii) Asymmetric: Two amide NH groups of a molecule oriented along one direction and the third in the opposite direction (hereinafter referred to as 2:1). A dimer of this type is shown in Figure 6b.

Once a 2:1 dimer is formed, any other molecule hydrogen bonds to this dimer in the same asymmetric fashion, resulting in a columnar stack which is entirely constituted by hydrogen bonds of the 2:1 type. Such stacks were formed in simulations carried out with either DREIDING-N and DREIDING-C force fields. The only manner in which an initially established 2:1 character cannot propagate is through a defect—a site where there are fewer than three intermolecular hydrogen bonds.

Could the formation of stacks in the 2:1 configuration be due to inadequate sampling or inadequacy of force fields? In the following, we examine this question and show that it is indeed more stable energetically than the 3:0 configuration.

Investigations of 2:1 Stacks. *Gas Phase Calculations.* Gas phase, zero Kelvin calculations of binding energies of geometry optimized oligomers of 2:1 and 3:0 stacks can provide an idea of their intrinsic stabilities. These were carried out using both varieties of the DREIDING force field, and the results are displayed in Table S1 (Supporting Information). Binding energies are marginally larger for the 2:1 stack

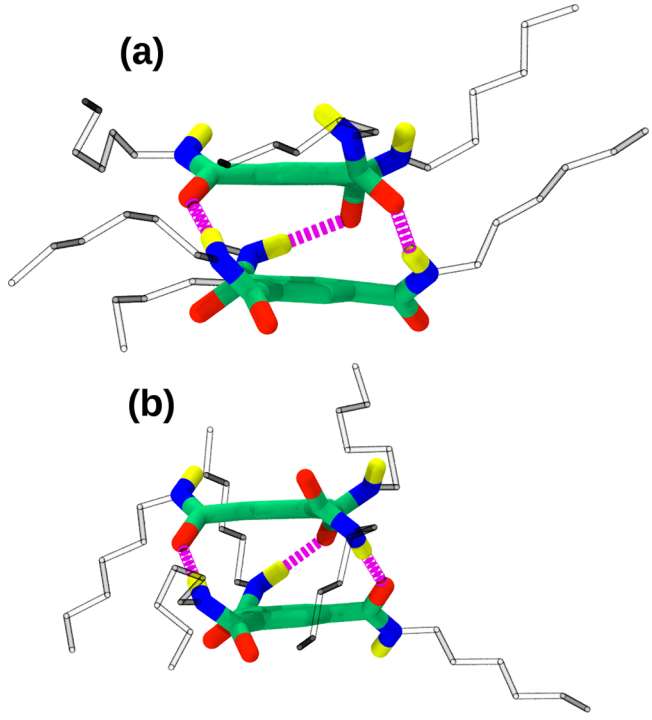

Figure 6. Two different configurations of **1c** dimer: (a) 3:0 (alias symmetric); (b) 2:1 (alias asymmetric).

dx.doi.org/10.1021/jp502779z | J. Phys. Chem. B 2014, 118, 5218−5228

compared to that for the 3:0 stack. Both stacking patterns exhibit cooperativity in binding energy, as shown in Figure 7.

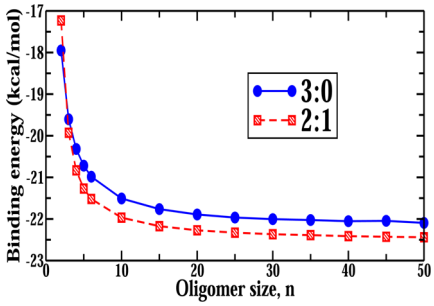

Figure 7. Cooperativity in binding energy exhibited by gas-phase geometry optimized oligomers of **1a** for 3:0 and 2:1 types of stacking obtained using the DREIDING-C force field.

Quantum Chemical Calculations. It is interesting that, in both varieties of the DREIDING force field, the binding energies of a 2:1 stack are marginally higher (in magnitude) than the corresponding 3:0 one. Earlier quantum chemical studies had exclusively examined the 3:0 stacks only.[16,17,49] Thus, we have carried out gas phase density functional theory (DFT) based quantum chemical calculations at the B3LYP/6-311+g(d,p) level of theory for a few oligomers of **1a** in both 2:1 and 3:0 configurations using GAUSSIAN-09[50] and NWChem.[51] While the M06-2X + DFT-D3 calculations were carried out using NWChem, the B3LYP ones were performed using GAUSSIAN-09. Table 2 shows the binding energy of geometry optimized 2:1 oligomers to be larger than that of 3:0 stacks at both levels of quantum theory, consistent with the results from the DREIDING force fields.

The replacement of an amide proton with a methyl group does not affect the relative stabilities of the two stacking types, and the 2:1 dimer is found to be more stable than the 3:0 one by 2.52 kcal/mol at the B3LYP/6-311+g(d,p) level of theory. In an earlier study, Schmidt and co-workers compared the heats of formation for the two types of stacks using a semiempirical PM6 model.[25] For the BTA trimer with methyl tails, they observed the heat of formation for the 2:1 stacking type to be greater than that of the 3:0 one by around 30 kJ/mol, which is very much consistent with results from our DFT calculations. The above analyses show that oligomers of the 2:1 type are more stable than the corresponding 3:0 stacks. Furthermore, for a given length of the alkyl tail of BTA, the difference in stability increases with oligomer size.

The stability of the 2:1 oligomer relative to that of the 3:0 one can be explained as follows: Each intermolecular hydrogen bond possesses a dipole moment oriented from the carbonyl oxygen of one molecule to the amide hydrogen of another. Classical electrostatic interaction between these dipoles demands an antiparallel arrangement to be the energetically favored configuration. Given that there are three hydrogen bonds between a pair of molecules, not all of the three dipole−dipole configurations can be antiparallel, a situation which is similar to the frustrated antiferromagnetic configuration of spins on a triangular lattice. Thus, one hydrogen bond dipole flips to provide two antiparallel interactions. This is one of the causes for the stabilization of the 2:1 stack, and the same was alluded to earlier by Schmidt and co-workers.[25] The difference in the energies of a 3:0 and a 2:1 dimer should thus be 4*E*, where *E* is the dipole−dipole interaction energy between proximal intermolecular hydrogen bonds. On the basis of the atom charges (of the Dreiding force field) and the distances in the optimized dimer configurations, we estimate *E* to be around 0.25 kcal/mol. Thus, the difference in energies between 3:0 and 2:1 dimers is estimated to be around 1.0 kcal/mol which is in the same scale as the value of 3.46 kcal/mol, the difference between 3:0 and 2:1 dimer energies.

The energy difference between the two kinds of dimers will depend on the length of the alkyl tail. To investigate this aspect, dimers of 2:1 and 3:0 types for different alkyl tail lengths were geometry optimized. The difference in the energies between the two dimers decreases with increasing tail length up to a length of four, beyond which it saturates to a value around 2 kcal/mol (favoring the 2:1 configuration), as shown in Table 3. The energy difference between the two stacking types can be attributed to differences in the van der Waals interactions between the tails. The most favored distance between intermolecular CH_2 groups in *n*-alkanes is 4.5 Å. The 2:1 type stacking has fewer CH_2 pairs at such a distance than the 3:0 one. This difference is the underlying reason for the decrease in the relative stability of the 2:1 dimer over the 3:0 one. However, since the alkyl groups attached to the two

Table 3. Energy Difference ($E_{3:0} - E_{2:1}$) (in kcal/mol) between Geometry Optimized Dimers of BTA Possessing Different Alkyl Tails Using the B3LYP/6-311+g(d,p) Level of Theory

alkyl tail (R)	Δ*E*
hydrogen	2.82
methyl	2.52
propyl	1.87
butyl	1.87
pentyl	2.13

Table 2. Energy Difference ($E_{3:0} - E_{2:1}$) (in kcal/mol) between Optimized Geometries of 3:0 and 2:1 Type BTA Oligomers[a]

oligomer size (*n*)	B3LYP/6-311+g(d,p)	B3LYP/6-311+g(d,p)//B3LYP/cc-pVTZ	B3LYP/6-311+g(d,p)//M06-2X/cc-pvTZ + DFT-D3
		R = Hydrogen	
2	2.82	2.35	1.67
3	8.06	7.58	7.45
4	11.60	11.31	10.28
		R = Methyl	
2	2.52	2.07	0.62
3	7.94	7.48	6.37
4	11.55	11.29	10.36

[a]See Figure S1 (Supporting Information) for the molecular structures.

dx.doi.org/10.1021/jp502779z | J. Phys. Chem. B 2014, 118, 5218−5228

molecules in a dimer have a relative angle of 60° (see Figure 6), this difference in CH_2 pair distances does not propagate beyond four carbon atoms in the alkyl chain. Thus, the $E_{3:0} - E_{2:1}$ saturates beyond R = butyl. Inclusion of zero point energy (ZPE) for the dimers with R = H and R = methyl does not significantly alter the energy difference. $E_{3:0} - E_{2:1}$ including the ZPE reduces marginally to values of 2.26 kcal/mol (R = H) and 2.13 kcal/mol (R = Me). The free energy difference (with contributions from vibrational, rotational, and electronic degrees of freedom) at 298.15 K calculated within the B3LYP/6-311+g(d,p) level of theory too favors the 2:1 dimer for both R = H (+1.76 kcal/mol) and R = Me (+1.52 kcal/mol). Thus, it is likely that the stability of the 2:1 dimer over the 3:0 one observed here is reliable.

Crystal structures[52−54] of BTA with *n*-alkyl tails (*n* = 1, 2, 3, 8) exhibit sheet-like geometries instead of the one-dimensional structures expected in solution and studied herein. Thus, a direct comparison of the 2:1 stacking type with the molecular packing in the crystal is not possible. Only one crystal structure with one-dimensional stacking feature is known but for R = methoxyethyl. This structure exhibits 3-fold hydrogen bonds between π stacked molecules, and the hydrogen bonds are of 3:0 type.[46] We presume that the ether linkage is responsible for the stabilization of the 3:0 geometry in this case.

2:1 and 3:0 Stacks in Solvent. MD simulations of a 20-mer stacked in either 2:1 or 3:0 fashion were carried out in bulk *n*-nonane at 298.15 K in the NPT ensemble for a duration of 5 ns. Intermolecular hydrogen bonds in both of the stacks were seen to be preserved in these simulations. Thus, the nature of the stack (i.e., either 2:1 or 3:0 type) did not change during the course of the MD trajectory. The mean potential energy of a molecule in a stack was calculated as described earlier and is shown in Figure S3a (Supporting Information) as a function of time. Again, a molecule belonging to the 2:1 stack is found to be more stable than one present in the 3:0 one. The mean potential energy difference between a molecule present in these stacks is around 11.5 kcal/mol under ambient conditions. *It is to be noted that a 2:1 stack can be realized in three different ways versus the single realization of a stack in the 3:0 manner.* Thus, the former is stabilized by entropic grounds, in addition to energetic reasons, making the 2:1 stack thermodynamically more stable than the corresponding 3:0 stack. We have also performed calculations to estimate the dihedral barrier for the transformation of a molecule between the 3:0 and 2:1 structures, the results of which are discussed in the Supporting Information (Figure S2).

The macrodipole of the stacks (Figure S3b, Supporting Information) fluctuates in time about a mean value, due to its flexibility. As expected, the 3:0 stack possesses a larger dipole moment (almost thrice) than the 2:1 stack. The amplitude of fluctuations will decrease with an increase in stack size.

Free Energy Calculations. Meijer and co-workers[55,56] have developed theoretical models to describe the thermodynamics of self-assembly of several systems similar to that studied here. Enthalpy release, temperature of elongation, and change in entropy can be obtained using these models. Until now, the FE of oligomerization of BTA in a solvent has not been studied using atomistic simulations. Thus, we have carried out FE calculations based on the ABF method to investigate its dimerization and solvation free energies. Further, we have studied the effect of alkyl tail length on these quantities.

Dimerization in the Gas Phase and in Bulk Solvent. The FE of dimerization in the gas phase was calculated in the NVT ensemble at 298.15 K using both varieties of the DREIDING force field. As mentioned earlier, the RC was split into four windows and MD simulations were carried out for 25 ns in each window to ensure the convergence of FE. The gas phase DFE profiles of **1a**, **1b**, and **1c** are shown in Figure S4 (Supporting Information), and the values are given in Table 4.

Table 4. Dimerization (DFE) and Solvation Free Energies (SFE) (in kcal/mol) of 1a, 1b, and 1c at 298.15 K

molecule	DREIDING-N	DREIDING-C
	DFE (gas phase)	
1a	−12.01	−7.08
1b	−17.68	−18.90
1c	−19.22	−20.90
	DFE (in *n*-nonane)	
1a	−8.15	−9.24
1b	−10.17	−11.67
1c	−10.18	−12.81
	SFE	
1a	−2.07	−3.24
1b	−12.71	−10.39
1c	−20.33	−19.47

Increasing the length of the alkyl chain results in an increase in the stabilization of the dimer with respect to two monomers, as studied through both the DREIDING-N and DREIDING-C force fields. The dimer of **1a** in the gas phase is found to be not stable within the DREIDING-C force field. The force field has a specific potential term for the hydrogen bond interaction which contains an inner and outer distance cutoff. The oscillations in the profiles are due to the break in the intermolecular hydrogen bonds, and the consequent inactivation of this potential term.

To determine the DFE in *n*-nonane, MD simulations were carried out in the constant NPT ensemble at 298.15 K. Each window was run for 35 ns, and a total trajectory of 140 ns was generated to obtain the FE profile for **1c**. The dimerization FE in solvent is smaller than that in the gas phase, as expected. Further, solvent molecules penetrate between the two BTA molecules, which results in the realization of the monomer state at a shorter distance compared to that in the gas phase (see Figure 8).

The DFE profiles for BTA in solvent are displayed in Figure 9, and the values are given in Table 4. While the self-assembly of **1a** appears to not be feasible in the solvent, those of **1b** and **1c** are, signifying the importance of the additional stabilization offered by the alkyl groups to the dimer.

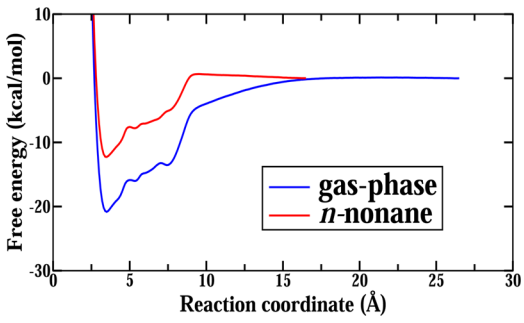

Figure 8. Comparison of dimerization free energy profiles of **1c** in the gas phase and in bulk *n*-nonane at 298.15 K.

dx.doi.org/10.1021/jp502779z | J. Phys. Chem. B 2014, 118, 5218−5228

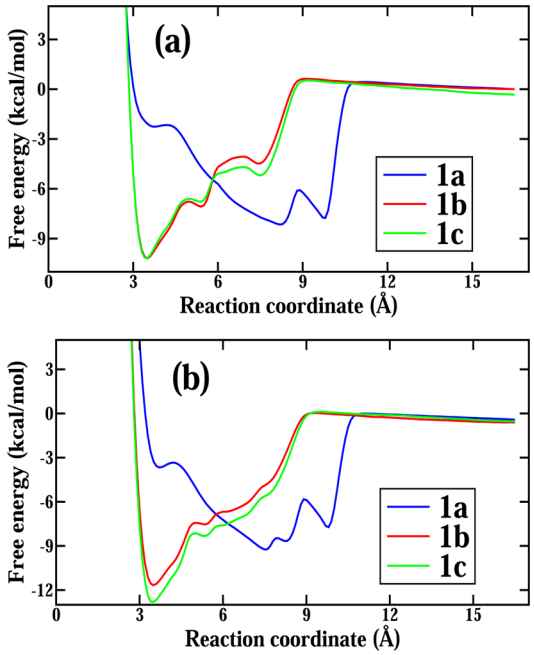

Figure 9. Dimerization free energy profiles in bulk *n*-nonane at 298.15 K obtained using the (a) DREIDING-N and (b) DREIDING-C force fields.

Solvation Free Energy (SFE). SFE quantifies the stability offered by the solvent to a BTA molecule with respect to its state in the gas phase. SFE profiles are shown in Figure 10, and the values are given in Table 4. The change in the FE as the molecule enters the solvent is gradual and converges when it is completely solvated. The range over which the FE varies increases with molecular size. While BTA molecules with longer alkyl groups tend to enter the solvent end-on, few solvent molecules too were seen to rise out of the planar liquid–vapor interface to interact with such alkyl groups of BTA. These events increase the range over which SFE varies. All BTA molecules are stabilized in *n*-nonane compared to the gas phase. SFE increases with an increase in the alkyl group length due to the increase in van der Waals interactions between the alkyl tails and nonane molecules. The solvation FE of a dimer can be obtained from that of the monomer and the dimerization FE profiles using a Born–Haber cycle (Figure S5, Supporting Information), and the results are shown in Table S2 (Supporting Information).

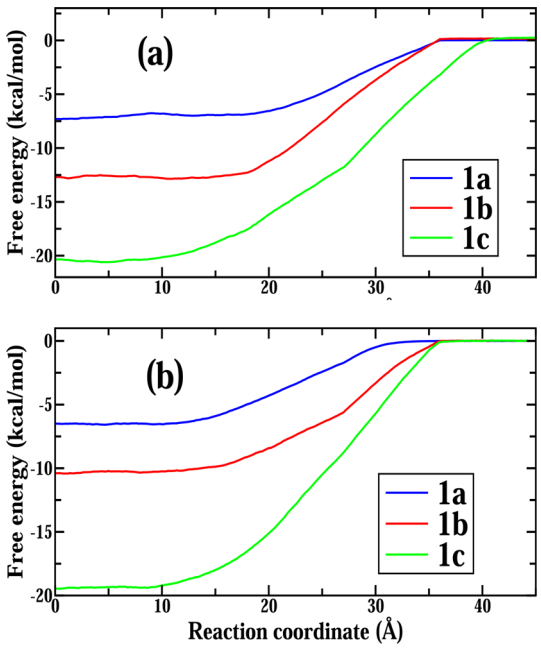

Figure 10. Solvation free energy profiles of BTA from a vacuum (large distances) to bulk *n*-nonane at 298.15 K studied using the (a) DREIDING-N and (b) DREIDING-C force fields.

Cooperativity Examined through Free Energy. As discussed above, the self-assembly of BTA molecules proceeds via a cooperative mechanism. The strength with which each molecule binds to an existing stack increases with oligomer size; relative to a monomer, a molecule present in a dimer has a lower FE than one which is part of a larger oligomer, say a decamer. This aspect has earlier been probed by us and others using quantum chemical methods in the gas phase at zero Kelvin temperature.[16,17,25,49] In the current manuscript, the same was studied using force fields (see Figure 7). Herein, we present a demonstration of the cooperative nature of self-assembly of BTA in solution, under ambient conditions. ABF calculations were used to calculate the FE profiles for the removal of one BTA molecule from three oligomers of **1c**—dimer, tetramer, and decamer.

The dimer, tetramer, and decamer of **1c** BTA were solvated in a pre-equilibrated box containing 500, 750, and 2000 *n*-nonane molecules, respectively. For all three systems, RC was defined as the distance between the centers of mass of the two BTA molecules which lie on the exterior of the stack (excluding its alkyl tails). Two collective variable (colvar) styles, "distanceZ" and "distanceXY", were used in evaluating the FE profiles. DistanceXY is used to restrict the BTA molecule to lie within a cylinder defined coaxially along the stack. The RC, "distanceZ" is the distance between the BTA molecule in one exterior of the stack and the center of mass of its immediate neighbor that is present in the stack. It was divided into three nonoverlapping windows with $N_{samples}$ as 2000 and bin width as 0.1 Å. Each window was run for 25 ns, and the convergence of FE was ascertained. Figure 11 clearly exhibits the cooperative behavior of assembly in the FE profiles.

The energy needed to remove a molecule from a decamer of **1c** is calculated to be 16.6 kcal/mol, while the corresponding values from a tetramer and dimer are 15.3 and 12.8 kcal/mol, respectively. In other words, the larger the oligomer size, the

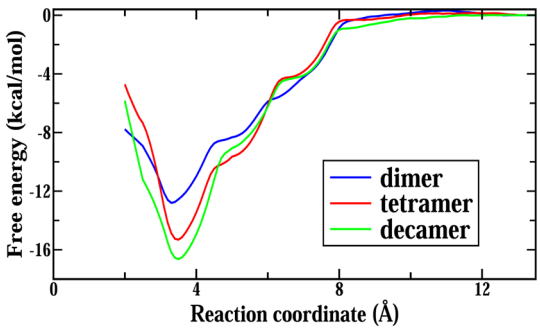

Figure 11. Free energy profiles for the release of a molecule from a dimer, tetramer, and decamer of **1c** solvated in *n*-nonane at 298.15 K. The reaction coordinate is the distance between the center of mass of the released molecule with respect to the center of mass of the next molecule present in the oligomer.

dx.doi.org/10.1021/jp502779z | J. Phys. Chem. B 2014, 118, 5218–5228

greater is the binding strength of a molecule in solvent, under ambient conditions.

CONCLUSIONS

Atomistic molecular dynamics simulations using two variants of the DREIDING force field[36] have been carried out to establish the nature of cooperative interactions that occur during the self-assembly of BTA in the solvent *n*-nonane under ambient conditions, and as a function of the length of its pendant alkyl groups. Cooperativity in binding energy has so far been reported only for small gas phase oligomers at zero Kelvin, using quantum chemical calculations.[16,17,25,49] Our main finding is that cooperative self-assembly is observed even using a nonpolarizable force field, not only in terms of the gas phase binding energy but also under experimentally relevant thermodynamic conditions, i.e., for the potential energy with increasing oligomer size in the solvent, and the free energy for the release of a BTA molecule from an oligomer.

Importantly, the self-assembly of BTA molecules from an arbitrarily dispersed configuration in *n*-nonane to a columnar stack has been demonstrated using atomistic MD simulations. The formation of a stack is seen to occur on a time scale of tens of nanoseconds. A key structural feature is the asymmetric intermolecular hydrogen bonding; i.e., a given BTA molecule forms two donor and one acceptor type hydrogen bond with a neighbor, which we denoted here as a 2:1 oligomer rather than a 3:0 oligomer, which has three donor and zero acceptor hydrogen bonds. 2:1 oligomers are found to be more stable than their 3:0 counterparts as studied using the DREIDING force field as well as through quantum density functional theory calculations. The stabilization is due to favorable antiparallel alignment of hydrogen bond dipole moments in the 2:1 state. Our calculations and simulations suggest the possibility of this configuration to be the ground state; however, the energy difference between the 2:1 and 3:0 dimers is in the range of 1−2 kcal/mol. An unambiguous identification of the ground state would require further experiments[57] and better quantum methods.

The dimerization free energy profile of BTA as well as its solvation free energy profile in *n*-nonane have been determined using force field based simulations. The solvated dimer of **1c** (BTA with hexyl tails) is more stable than two of its solvated monomers by 12.8 kcal/mol. The solvation FE for the same compound is calculated to be −19.5 kcal/mol. These values increase with increasing length of the alkyl group.

The FE profiles calculated here will be useful benchmarks for the development of a coarse grained (CG) model for BTA. Such an approach has been accomplished in other systems earlier.[58−63] In the present context, a CG model could be used to study the mechanism of not only columnar self-assembly but also fiber formation, which is of direct relevance to contemporary experiments.[22,64] In principle, this approach could be extended to molecules that self-assemble via an isodesmic mechanism as well. MD simulations based on chemically specific CG models should be able to delineate microscopic events and energetics of these two contrasting mechanisms that are operative in supramolecular polymerization. To this end, the development of CG models, in particular for BTA, and in general for other molecules exhibiting supramolecular polymerization, is currently underway in our group. These CG models will greatly extend the length and time scales of MD simulations beyond that undertaken here. The switching of the macrodipole moment of fibers upon the application of an external electric field[48] is another aspect that is worthy of study using molecular simulations.

ASSOCIATED CONTENT

Supporting Information

Binding energies of oligomers of 3:0 and 2:1 obtained through two variants of the DREIDING force field and the dihedral free energy barrier between the symmetric and asymmetric configurations are provided. The relative stability of 2:1 versus 3:0 dimers in solvent is also discussed. The Born−Haber cycle was employed to determine the solvation free energy of the dimer. Coordinates of all geometry optimized oligomers using quantum chemical methods are provided. This material is available free of charge via the Internet at http://pubs.acs.org.

AUTHOR INFORMATION

Corresponding Author

*E-mail: bala@jncasr.ac.in.

Notes

The authors declare no competing financial interest.

ACKNOWLEDGMENTS

K.K.B. and S.B. thank Chidambar Kulkarni and Dr. Subi George for useful discussions. K.K.B. thanks CSIR, India, for a senior research fellowship. S.B. thanks Sheikh Saqr Laboratory, JNCASR, for a senior fellowship.

REFERENCES

(1) Steed, J. W.; Atwood, J. L. *Supramolecular Chemistry*; John Wiley & Sons, Ltd.: West Sussex, United Kingdom, 2009.

(2) Matsunaga, Y.; Nakayasu, Y.; Sakai, S.; Yonenaga, M. Liquid Crystal Phases Exhibited by N,N′,N″-Trialkyl-1,3,5-Benzenetricaboxamides. *Mol. Cryst. Liq. Cryst.* **1986**, *141*, 327−333.

(3) van Bommel, K. J. C.; van der Pol, C.; Muizebelt, I.; Friggeri, A.; Heeres, A.; Meetsma, A.; Feringa, B. L.; van Esch, J. Responsive Cyclohexane-Based Low-Molecular-Weight Hydrogelators with Modular Architecture. *Angew. Chem., Int. Ed.* **2004**, *43*, 1663−1667.

(4) Wasielewski, M. R. Self-Assembly Strategies for Integrating Light Harvesting and Charge Separation in Artificial Photosynthetic Systems. *Acc. Chem. Res.* **2009**, *42*, 1910−1921.

(5) Fitié, C. F. C.; Roelofs, W. S. C.; Kemerink, M.; Sijbesma, R. P. Remnant Polarization in Thin Films from a Columnar Liquid Crystal. *J. Am. Chem. Soc.* **2010**, *132*, 6892−6893.

(6) Stals, P. J. M.; Smulders, M. M. J.; Martín-Rapún, R.; Palmans, A. R. A.; Meijer, E. W. Asymmetrically Substituted Benzene-1,3,5-tricarboxamides: Self-Assembly and Odd-Even Effects in the Solid State and in Dilute Solution. *Chem.—Eur. J.* **2009**, *15*, 2071−2080.

(7) Wang, F.; Gillissen, M. A. J.; Stals, P. J. M.; Palmans, A. R. A.; Meijer, E. W. Hydrogen Bonding Directed Supramolecular Polymerisation of Oligo(Phenylene-Ethynylene)s: Cooperative Mechanism, Core Symmetry Effect and Chiral Amplification. *Chem.—Eur. J.* **2012**, *18*, 11761−11770.

(8) Narayan, B.; Kulkarni, C.; George, S. J. Synthesis and self-assembly of a C3-symmetric benzene-1,3,5-tricarboxamide (BTA) anchored naphthalene diimide disc. *J. Mater. Chem. C* **2013**, *1*, 626−629.

(9) Percec, V.; Imam, M. R.; Peterca, M.; Wilson, D. A.; Graf, R.; Spiess, H. W.; Balagurusamy, V. S. K.; Heiney, P. A. Self-Assembly of Dendronized Triphenylenes into Helical Pyramidal Columns and Chiral Spheres. *J. Am. Chem. Soc.* **2009**, *131*, 7662−7677.

(10) Percec, V.; Peterca, M.; Tadjiev, T.; Zeng, X.; Ungar, G.; Leowanawat, P.; Aqad, E.; Imam, M. R.; Rosen, B. M.; Akbey, U.; et al. Self-Assembly of Dendronized Perylene Bisimides into Complex Helical Columns. *J. Am. Chem. Soc.* **2011**, *133*, 12197−12219.

(11) Smulders, M. M. J.; Schenning, A. P. H. J.; Meijer, E. W. Insight into the Mechanisms of Cooperative Self-Assembly: The "Sergeants-and-Soldiers" Principle of Chiral and Achiral C3-Symmetrical Discotic Triamides. *J. Am. Chem. Soc.* **2008**, *130*, 606−611.
(12) Palmans, A. R. A.; Meijer, E. W. Amplification of Chirality in Dynamic Supramolecular Aggregates. *Angew. Chem., Int. Ed.* **2007**, *46*, 8948−8968.
(13) Kulkarni, C.; Munirathinam, R.; George, S. J. Self-Assembly of Coronene Bisimides: Mechanistic Insight and Chiral Amplification. *Chem.—Eur. J.* **2013**, *19*, 11270−11278.
(14) Kumar, M.; Jonnalagadda, N.; George, S. J. Molecular recognition driven self-assembly and chiral induction in naphthalene diimide amphiphiles. *Chem. Commun.* **2012**, *48*, 10948−10950.
(15) De Greef, T. F. A.; Smulders, M. M. J.; Wolffs, M.; Schenning, A. P. H. J.; Sijbesma, R. P.; Meijer, E. W. Supramolecular Polymerization. *Chem. Rev.* **2009**, *109*, 5687−5754.
(16) Kulkarni, C.; Reddy, S. K.; George, S. J.; Balasubramanian, S. Cooperativity in the stacking of benzene-1,3,5-tricarboxamide: The role of dispersion. *Chem. Phys. Lett.* **2011**, *515*, 226−230.
(17) Filot, I. A. W.; Palmans, A. R. A.; Hilbers, P. A. J.; van Santen, R. A.; Pidko, E. A.; de Greef, T. F. A. Understanding Cooperativity in Hydrogen-Bond-Induced Supramolecular Polymerization: A Density Functional Theory Study. *J. Phys. Chem. B* **2010**, *114*, 13667−13674.
(18) Kulkarni, C.; Balasubramanian, S.; George, S. J. What Molecular Features Govern the Mechanism of Supramolecular Polymerization? *ChemPhysChem* **2013**, *14*, 661−673.
(19) Nakano, Y.; Markvoort, A. J.; Cantekin, S.; Filot, I. A. W.; ten Eikelder, H. M. M.; Meijer, E. W.; Palmans, A. R. A. Conformational Analysis of Chiral Supramolecular Aggregates: Modeling the Subtle Difference between Hydrogen and Deuterium. *J. Am. Chem. Soc.* **2013**, *135*, 16497−16506.
(20) Korevaar, P. A.; Schaefer, C.; de Greef, T. F. A.; Meijer, E. W. Controlling Chemical Self-Assembly by Solvent-Dependent Dynamics. *J. Am. Chem. Soc.* **2012**, *134*, 13482−13491.
(21) Cantekin, S.; de Greef, T. F. A.; Palmans, A. R. A. Benzene-1,3,5-tricarboxamide: a versatile ordering moiety for supramolecular chemistry. *Chem. Soc. Rev.* **2012**, *41*, 6125−6137.
(22) Stals, P. J. M.; Korevaar, P. A.; Gillissen, M. A. J.; de Greef, T. F. A.; Fitié, C. F. C.; Sijbesma, R. P.; Palmans, A. R. A.; Meijer, E. W. Symmetry Breaking in the Self-Assembly of Partially Fluorinated Benzene-1,3,5-tricarboxamides. *Angew. Chem., Int. Ed.* **2012**, *51*, 11297−11301.
(23) Cantekin, S.; Nakano, Y.; Everts, J. C.; van der Schoot, P.; Meijer, E. W.; Palmans, A. R. A. A stereoselectively deuterated supramolecular motif to probe the role of solvent during self-assembly processes. *Chem. Commun.* **2012**, *48*, 3803−3805.
(24) Brunsveld, L.; Schenning, A. P. H. J.; Broeren, M. A. C.; Janssen, H. M.; Vekemans, J. A. J. M.; Meijer, E. W. Chiral Amplification in Columns of Self-Assembled N,N′,N″-Tris((S)-3,7-dimethyloctyl)-benzene-1,3,5-tricarboxamide in Dilute Solution. *Chem. Lett.* **2000**, *29*, 292−293.
(25) Albuquerque, R. Q.; Timme, A.; Kress, R.; Senker, J.; Schmidt, H.-W. Theoretical Investigation of Macrodipoles in Supramolecular Columnar Stackings. *Chem.—Eur. J.* **2013**, *19*, 1647−1657.
(26) Klein, M. L.; Shinoda, W. Large-Scale Molecular Dynamics Simulations of Self-Assembling Systems. *Science* **2008**, *321*, 798−800.
(27) Yu, T.; Lee, O.-S.; Schatz, G. C. Steered Molecular Dynamics Studies of the Potential of Mean Force for Peptide Amphiphile Self-Assembly into Cylindrical Nanofibers. *J. Phys. Chem. A* **2013**, *117*, 7453−7460.
(28) Yu, T.; Schatz, G. C. Free Energy Profile and Mechanism of Self-Assembly of Peptide Amphiphiles Based on a Collective Assembly Coordinate. *J. Phys. Chem. B* **2013**, *117*, 9004−9013.
(29) Lee, O.-S.; Stupp, S. I.; Schatz, G. C. Atomistic Molecular Dynamics Simulations of Peptide Amphiphile Self-Assembly into Cylindrical Nanofibers. *J. Am. Chem. Soc.* **2011**, *133*, 3677−3683.
(30) Das, J.; Eun, C.; Perkin, S.; Berkowitz, M. L. Restructuring of Hydrophobic Surfaces Created by Surfactant Adsorption to Mica Surfaces. *Langmuir* **2011**, *27*, 11737−11741.
(31) Santo, K. P.; Berkowitz, M. L. Difference between Magainin-2 and Melittin Assemblies in Phosphatidylcholine Bilayers: Results from Coarse-Grained Simulations. *J. Phys. Chem. B* **2012**, *116*, 3021−3030.
(32) Jeon, J.; Mills, C. E.; Shell, M. S. Molecular Insights into Diphenylalanine Nanotube Assembly: All-Atom Simulations of Oligomerization. *J. Phys. Chem. B* **2013**, *117*, 3935−3943.
(33) Danila, I.; Riobé, F.; Piron, F.; Puigmartí-Luis, J.; Wallis, J. D.; Linares, M.; Ågren, H.; Beljonne, D.; Amabilino, D. B.; Avarvari, N. Hierarchical Chiral Expression from the Nano- to Mesoscale in Synthetic Supramolecular Helical Fibers of a Nonamphiphilic C3-Symmetrical π-Functional Molecule. *J. Am. Chem. Soc.* **2011**, *133*, 8344−8353.
(34) Chami, F.; Wilson, M. R. Molecular Order in a Chromonic Liquid Crystal: A Molecular Simulation Study of the Anionic Azo Dye Sunset Yellow. *J. Am. Chem. Soc.* **2010**, *132*, 7794−7802.
(35) Brocorens, P.; Linares, M.; Guyard-Duhayon, C.; Guillot, R.; Andrioletti, B.; Suhr, D.; Isare, B.; Lazzaroni, R.; Bouteiller, L. Conformational Plasticity of Hydrogen Bonded Bis-urea Supramolecular Polymers. *J. Phys. Chem. B* **2013**, *117*, 5379−5386.
(36) Mayo, S. L.; Olafson, B. D.; Goddard, W. A. DREIDING: a generic force field for molecular simulations. *J. Phys. Chem.* **1990**, *94*, 8897−8909.
(37) Gasteiger, J.; Marsili, M. Iterative partial equalization of orbital electronegativity-a rapid access to atomic charges. *Tetrahedron* **1980**, *36*, 3219−3228.
(38) Plimpton, S. Fast Parallel Algorithms for Short-Range Molecular Dynamics. *J. Comput. Phys.* **1995**, *117*, 1−19.
(39) Martyna, G. J.; Klein, M. L.; Tuckerman, M. Nosé-Hoover chains: The canonical ensemble via continuous dynamics. *J. Chem. Phys.* **1992**, *97*, 2635−2643.
(40) Hockney, R. W.; Eastwood, J. W. *Computer Simulation Using Particles*; Taylor & Francis: Bristol, USA, 1988.
(41) Martin, M. G.; Siepmann, J. I. Transferable Potentials for Phase Equilibria. 1. United-Atom Description of n-Alkanes. *J. Phys. Chem. B* **1998**, *102*, 2569−2577.
(42) Tuckerman, M.; Berne, B. J.; Martyna, G. J. Reversible multiple time scale molecular dynamics. *J. Chem. Phys.* **1992**, *97*, 1990−2001.
(43) Humphrey, W.; Dalke, A.; Schulten, K. VMD − Visual Molecular Dynamics. *J. Mol. Graphics* **1996**, *14*, 33−38.
(44) Darve, E.; Rodríguez-Gómez, D.; Pohorille, A. Adaptive biasing force method for scalar and vector free energy calculations. *J. Chem. Phys.* **2008**, *128*, 144120.
(45) Fiorin, G.; Klein, M.; Hénin, J. Using collective variables to drive molecular dynamics simulations. *Mol. Phys.* **2013**, *111*, 3345−3362.
(46) Lightfoot, M. P.; Mair, F. S.; Pritchard, R. G.; Warren, J. E. New supramolecular packing motifs: π-stacked rods encased in triply-helical hydrogen bonded amide strands. *Chem. Commun.* **1999**, 1945−1946.
(47) Martínez, L.; Andrade, R.; Birgin, E. G.; Martínez, J. M. PACKMOL: A package for building initial configurations for molecular dynamics simulations. *J. Comput. Chem.* **2009**, *30*, 2157−2164.
(48) Fitié, C. F. C.; Roelofs, W. S. C.; Magusin, P. C. M. M.; Wübbenhorst, M.; Kemerink, M.; Sijbesma, R. P. Polar Switching in Trialkylbenzene-1,3,5-tricarboxamides. *J. Phys. Chem. B* **2012**, *116*, 3928−3937.
(49) Smulders, M. M. J.; Buffeteau, T.; Cavagnat, D.; Wolffs, M.; Schenning, A. P. H. J.; Meijer, E. W. C3-symmetrical self-assembled structures investigated by vibrational circular dichroism. *Chirality* **2008**, *20*, 1016−1022.
(50) Frisch, M. J.; Trucks, G. W.; Schlegel, H. B.; Scuseria, G. E.; Robb, M. A.; Cheeseman, J. R.; Scalmani, G.; Barone, V.; Mennucci, B.; Petersson, G. A.; et al. *Gaussian 09*, revision D.01; Gaussian, Inc.: Wallingford, CT, 2009.
(51) Valiev, M.; Bylaska, E. J.; Govind, N.; Kowalski, K.; Straatsma, T. P.; Dam, H. J. J. V.; Wang, D.; Nieplocha, J.; Apra, E.; Windus, T. L.; de Jong, W. A. NWChem: A comprehensive and scalable open-source solution for large scale molecular simulations. *Comput. Phys. Commun.* **2010**, *181*, 1477−1489.

(52) Hanabusa, K.; Koto, C.; Kimura, M.; Shirai, H.; Kakehi, A. Remarkable Viscoelasticity of Organic Solvents Containing Trialkyl-1,3,5-benzenetricarboxamides and Their Intermolecular Hydrogen Bonding. *Chem. Lett.* **1997**, *26*, 429−430.
(53) Jiménez, C. A.; Belmar, J. B.; Ortíz, L.; Hidalgo, P.; Fabelo, O.; Pasán, J.; Ruiz-Pérez, C. Influence of the Aliphatic Wrapping in the Crystal Structure of Benzene Tricarboxamide Supramolecular Polymers. *Cryst. Growth Des.* **2009**, *9*, 4987−4989.
(54) Hou, X.; Schober, M.; Chu, Q. A Chiral Nanosheet Connected by Amide Hydrogen Bonds. *Cryst. Growth Des.* **2012**, *12*, 5159−5163.
(55) Jonkheijm, P.; van der Schoot, P.; Schenning, A. P. H. J.; Meijer, E. W. Probing the Solvent-Assisted Nucleation Pathway in Chemical Self-Assembly. *Science* **2006**, *313*, 80−83.
(56) Markvoort, A. J.; ten Eikelder, H. M. M.; Hilbers, P. A. J.; de Greef, T. F. A.; Meijer, E. W. Theoretical models of nonlinear effects in two-component cooperative supramolecular copolymerizations. *Nat. Commun.* **2011**, *2*, 509.
(57) Wegner, M.; Dudenko, D.; Sebastiani, D.; Palmans, A. R. A.; de Greef, T. F. A.; Graf, R.; Spiess, H. W. The impact of the amide connectivity on the assembly and dynamics of benzene-1,3,5-tricarboxamides in the solid state. *Chem. Sci.* **2011**, *2*, 2040−2049.
(58) Bhargava, B. L.; Devane, R.; Klein, M. L.; Balasubramanian, S. Nanoscale organization in room temperature ionic liquids: a coarse grained molecular dynamics simulation study. *Soft Matter* **2007**, *3*, 1395−1400.
(59) DeVane, R.; Jusufi, A.; Shinoda, W.; Chiu, C.-c.; Nielsen, S. O.; Moore, P. B.; Klein, M. L. Parametrization and Application of a Coarse Grained Force Field for Benzene/Fullerene Interactions with Lipids. *J. Phys. Chem. B* **2010**, *114*, 16364−16372.
(60) DeVane, R.; Klein, M. L.; Chiu, C.-c.; Nielsen, S. O.; Shinoda, W.; Moore, P. B. Coarse-Grained Potential Models for Phenyl-Based Molecules: I. Parametrization Using Experimental Data. *J. Phys. Chem. B* **2010**, *114*, 6386−6393.
(61) Li, Z.; Wang, P.; Yan, Y.; Wang, R.; Zhang, J.; Dai, C.; Hu, S. Tuning and Designing the Self-Assembly of Surfactants: The Magic of Carbon Nanotube Arrays. *J. Phys. Chem. Lett.* **2013**, *4*, 3962−3966.
(62) He, J.; Huang, X.; Li, Y.-C.; Liu, Y.; Babu, T.; Aronova, M. A.; Wang, S.; Lu, Z.; Chen, X.; Nie, Z. Self-Assembly of Amphiphilic Plasmonic Micelle-Like Nanoparticles in Selective Solvents. *J. Am. Chem. Soc.* **2013**, *135*, 7974−7984.
(63) Schor, M.; Ensing, B.; Bolhuis, P. G. A simple coarse-grained model for self-assembling silk-like protein fibers. *Faraday Discuss.* **2010**, *144*, 127−141.
(64) Singer, J. C.; Giesa, R.; Schmidt, H.-W. Shaping self-assembling small molecules into fibres by melt electrospinning. *Soft Matter* **2012**, *8*, 9972−9976.